The Cool Oscillator Coupled-Energy-Mode Model for Advanced Performance Analysis and Prediction

Oscillator-Physics Reveals Chaotic Instabilities of Carrier Phase-Noise and Allan Variance

Michael J Underhill, Underhill Research Limited, Lingfield, UK
Email: mike@underhill.co.uk

***Summary*— Now that very low noise amplifiers are available the Cool-Oscillator and any of its variants are shown to predict typically up to 10 dB or so better performance than the Leeson model. The Cool oscillator model is now to be preferred for future oscillator design and assessment.**

In any oscillator model the spectra of the noise and signals at the input should always be combined 'vectorially' for both power and amplitude. This reveals the unstable parts of the oscillator spectrum. The instabilities appear at the 'corner' frequencies and times of both the spectrum and Allan Variance plots when represented by 'asymptotes'. And these 'metastable and 'chaotic' instabilities are estimated to be bounded in peak energy density and total noise energy by partial coupling to be < 2.5 % or $1/(2\pi)^2$ of the sideband energy density at 'corner-frequencies'.

Oscillator spectra can conveniently be represented by a pair of lower sideband (LSB) and upper sideband (USB) 'Coupled-Energy-Modes' (CEMs), recognizable as $L_{LSB}(f)$ and $L_{USB}(f)$. Then $S\phi(f)$ is the 'vector-addition' $\oplus$ of the two sideband Energy-Modes. CEMS can conveniently be represented as Energy/Power Laplace-Transforms with an individual mode energy assigned to each of them. And this allows oscillator switch-on and switch-off dynamics to be modeled. Also, partial-coupling between the two modes is what causes chaotic and metastable exchange of energy limited to about 2.5 %.

The 'corner-frequencies' on a spectrum plot with asymptotes can be directly related to the 'corner-times' on an asymptotic Allan Variance (AVAR) plot by reversing the AVAR plot left to right and suitably aligning the logarithmic scales with some small offsets predicted depending on the asymptotic slopes at each corner-point. Example measured plots for an NEL OCXO are shown to demonstrate this.

Also an asymptotic AVAR process 'filter' characteristic is shown to be constant in shape and size when plotted in the AVAR plot.

Keywords—cool-oscillator; oscillator-physics; coupled-energy-modes; phase-noise; Allan-variance; chaos; metastability; feed-back; energy transfer-functions; Laplace-transforms; partial fractions

I. Introduction

This paper re-examines several aspects of oscillator behavior and predicted and measured performance from the viewpoint of 'oscillator-physics'. Particularly that is how the energy of the oscillator is created, distributed in the frequency spectrum, built up, stored in, and dissipated from its resonator. This approach reveals that the original 'simple' Leeson model equation [1], its improved version put forward by Everard [2] [3] and further improved by Underhill as the Cool-Oscillator equation [4] can all be further improved by addressing oscillator physics together with feedback control system analysis [9, 10] using 'Laplace-transform' [8] 'partial-fraction' [12] type expressions for what are here called Coupled-Energy-Modes. By 'inverting' the Laplace-Transforms [11] the CEMs can predict the switch-on characteristics for any oscillator open loop gain and the switch-off decay characteristic of the oscillator resonator.

The CEM concept elaborates the concept of the simple single mode oscillator to the next level of two or more modes. The simple CEM model is represented by a pair of poles coupled together and being able to exchange energy between these 'modes' for a full range of phase differences, and within the constraint that the total spectrum energy is fixed. It is useful to think of the two modes being the upper and lower sidebands of the oscillator spectrum The spectrum shape and its fundamental instabilities can be translated into Allan-variance plots by the techniques indicated in Enrico Rubiola's Chart [7]. ng lower and upper sideband modes space about one oscillator bandwidth (~2α) apart.

The maximum energy exchange is limited by the coupling or degree of correlation between the two sidebands. This is estimated at about 2.5% from an examination of 'oscillator-physics' and oscillator measurements. The oscillator physics will be published in due course.

A useful discovery from the investigation of how two Gaussian noise signals combine is that the maximum energy exchange occurs only at the frequencies where the two spectra have equal amplitudes. And so this occurs at the 'corner frequencies of 'asymptotic spectra plots which it is shown that these correlate with the corner frequencies of Allan Variance plots. (A practical example of both of these taken from measurements of an NEL OCXO is given.

The control system approach in this paper has been developed over many years, from the late seventies to the present. The evidence for this can be by examining this author's references given in a separate list at the end of this paper. The list of fifty-five papers covers from 1978 to the present.

This control system approach is what has led to the discoveries of how chaotic instabilities can occur because the power level and hence the overall spectrum power of any oscillator is always constrained to a fixed value.

II. Oscillator Model Comparison – 'Leeson' and 'Cool'

Fig. 1 shows why the Cool oscillator gives a more accurate and less pessimist phase noise prediction the Leeson model now that very low noise amplifiers are available. The comparison assumes an amplifier with a noise-factor of 1.1 which corresponds to a noise-figure of 0.4 dB. The effective temperature T_e of the oscillator is then ten times lower than the ambient temperature T_a and the oscillator phase noise is improved by 10 dB.

This shows why the 'Cool' oscillator model is now to be preferred over the Leeson' model.

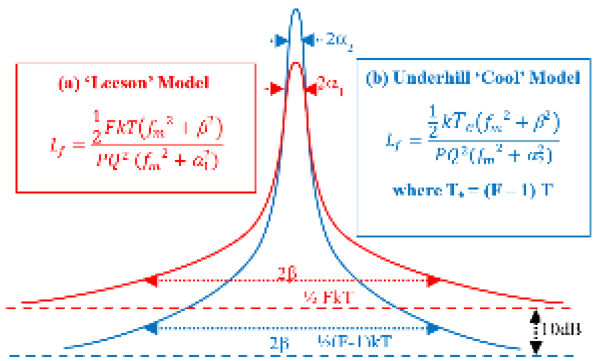

Fig. 1. Comparison of phase noise spectra of 'Leeson' and 'Cool' models for a mismatched voltage amplifier with NF of 1.1 (0.4dB). Note that the added noise at the amplifier input is (F-1)kT. L(f) is then improved by 10dB (10). The equivalent noise temperature Te = Tamb/10. The sideband frequency is f_m

III. Essential Physics and Mathematics of Summing Junction of any Oscillator Feedback Model

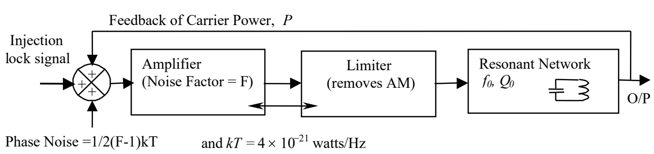

Feedback model of any oscillator but with three inputs to the summing junction and the 'Cool' correction to the amplifier input noise and equivalent temperature.

In Fig. 2 simple addition of the signals at the Summing Junction (P = P1 + P2 + P3) is found to be invalid physics even if the additions are averaged over a long time. The physics demands an summing process that takes into account the 'inter-coupling' and 'correlation' between all three signals and at every frequency.

'Vector-addition' taking account of relative phases of power densities over the frequency band of interest found to be the answer. Suitable representation using ⊕ to mean 'vector addition taking coupling correlation and phase into account' is

$$P(f) = P_1(f) \oplus P_2(f) \oplus P_3(f) \qquad (1a)$$

Or in more correct detail:

$$P(f) = \sqrt{[P_1(f)^2 \oplus P_2(f)^2 \oplus P_3(f)^2]} \qquad (1b)$$

In this way the Summing-Junction (at left) adds three signals which each can be 'noise' or 'discrete'.

Note that all oscillator spectra are white noise filtered by the very high Q, narrow bandwidth, of the resonator Q, Q being multiplied many times (~ 10^8 or so). Oscillator spectra can be considered to be 'totally phase-noise' and treated accordingly.

Furthermore, the addition process, by physics-definition has to be power/energy conserving as a long-term average. And this has consequences:

(a) Parts of two spectra may cancel at certain frequencies when the parts are nearly equal.

(b) The cancellation of two equal Gaussian signals creates non-Gaussian noise which can be 'metastable' and 'chaotic'.

Fortunately the worst case coupling which occurs at frequencies when the spectral densities are equal is estimated from the physics to be about $1/(2\pi)^2$ being about 2.5% or about 1.5 dB the this worst case frequency. And the error is bounded within an estimated fractional bandwidth of $\sim 1/(\pi) = 1/3.14 = 0.32$.

Thus, in summary the inescapable instabilities are small and only occur when noise process asymptotes cross at 'corner frequencies'.

IV. Laplace Variable Representations of Oscillator Spectrum and Dynamics

The simple expressions for the spectra of oscillators in terms of frequency differences as shown for example in the 'boxed' expressions in Fig. 1, can be made much more useful. The 'trick' is to replace all the frequency terms by complex frequencies all represented by the Laplace variable 's'. Equation (3) defines the necessary substitution.

$$\partial/\partial t = s = \sigma \pm j\omega = \sigma \pm 2\pi f \qquad (2)$$

where t is time, σ is the 'damping' representing the decay or build-up of oscillator/resonator amplitude, ω is the angular frequency in radians-per-second, f is the frequency and $j = \sqrt{(-1)}$.

On this basis we can simply replace f by 's' as all the 2π cancel out, except when plotting the spectrum. The spectrum then has to be converted back to Hz from radians-per-second by dividing by 2π.

In Fig. 1 the cool-oscillator phase noise spectrum has two poles at $f_m = \alpha$ and two zeros at $f_m = \beta$ and is given by given as

$$P \times L(f) = \frac{\frac{1}{2}kT_e(f_m{}^2+\beta^2)}{Q_u^2(f_m{}^2+\alpha^2)} \qquad (3)$$

The spectrum given in Fig 1 should use vector-addition ⊕ and then is

$$P \times L(f) = \frac{\frac{1}{2}kT_e(f_m{}^2\oplus\beta^2)}{Q_u^2(f_m{}^2\oplus\alpha^2)} \qquad (4)$$

And this can be converted into a per radian angular frequency power spectrum using vector addition ⊕ giving in the form

$$P \times L_{rad}(f) = (\tfrac{1}{2}\, kT_e/Q^2)(s^2 \oplus \beta^2)/(s^2 \oplus \alpha^2) \qquad (5)$$

Then (3) is in the form of a Laplace Transform that can be 'inverted' [11] to give the dynamics of the switch-on amplitude build-up and switch-off decay of the oscillator and its resonator.

The vector addition ⊕ that is used here also has the advantage that any spectrum can be separated into regions of interest around each of the corner-frequencies (as defined further below).

V. Lower and Upper Sideband Oscillator Energy-Modes

The vector addition ⊕ also should always be used when considering the upper and lower sidebands combine in a measurement of $S\phi(f)$ so that we have

$$S_\phi(f) = L_{LSB}(f) \oplus L_{USB}(f) \tag{6}$$

A useful discovery is that each L(f) can be regarded as a separate oscillator 'energy-modes' spaced symmetrically in frequency by no more than 2β the closed loop bandwidth of the oscillator. These are the two main 'Coupled-Energy-Modes' of any oscillator.

A small amount of energy (~2.5%) can then be exchanged (chaotically) between the two energy-modes provided that a total power/energy constraint is maintained. The constant power/energy constraint with κ as a 'coupling factor' ~2.5% is:

$$P^2 = P_1{}^2 + P_2{}^2 + \kappa^2 P_1 P_2 \tag{7}$$

Being at slightly different frequencies the relative phase of the oscillators can change to produce what might be called a 'beat frequency'. This clearly is an unstable situation with probable chaotic and metastable characteristics. Further investigation both theoretically and practically is needed to tie this down more precisely.

VI. Asymptotic Spectrum Representation

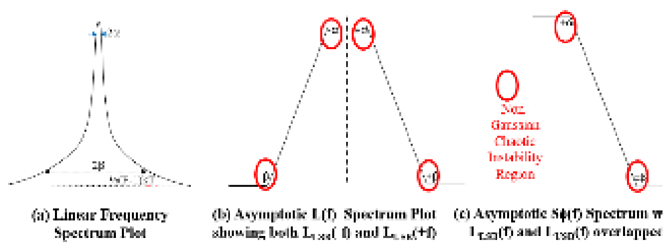

Fig. 2. **Spectrum Plots**. **(a) Linear:** 'Corner frequencies' are at ±α and ±β. **(b) Asymptotic L_{LSB}(f) and L_{USB}(f):** Vertical dashed line is 'overlap line' and overlap is chosen to show ±α 'corners.' T**(c) Asymptotic $S\phi(f) = L_{LSB}(f) \oplus L_{USB}(f)$:** The oscillator sidebands have varying amplitudes and phases and mix to cause small 'chaotic' (non-gaussian) instabilities at and around the 'corner-frequencies'.

Fig. 3 shows 'asymptotic' spectrum plots relating to the proposition there are (at least) two sideband energy modes for any oscillator. The sidebands L_{LSB}(f) and L_{USB}(f) of an oscillator are almost the same except at the 'corner frequencies' where about 2.5% of instability is a fundamental given from the physics of combining two almost equal amplitude Gaussian noise signals. This is shown where circled in red.

Also shown is how it is convenient to convert the linear spectra to a novel double-sided Bode plot [13] as shown in (b). Such a plot makes it easier to integrate any phase-noise spectrum without too much approximation to obtain the total phase noise power of the oscillator mode spectrum and then equate it to P.

The feature of the double sided Bode plot (b)is the there is an unavoidable overlap of the upper and lower sideband plots. This occurs at the central vertical dashed line. The make sure that all the important sideband feature are included the two corners at the top of the plot should be chosen to be sufficiently apart as shown.

We then find that the power P can divide chaotically between the two sideband modes. This is because of there is coupling κ between any pair of components as the result of the processes occurring in the summing junction of the oscillator The power equations are then of the form:

$$P^2 = P_1{}^2 + P_2{}^2 + \kappa^2 P_1 P_2 \tag{8}$$

where P1 and P2 are the powers of each mode/pole at any one time and $\kappa\sqrt{(P_1P_2)}$ is the power being exchanged at any one time, with κ as a coupling factor assumed between the two sideband modes.

VII. Aymptotic Spectrum and Allan Variance (ADEV) Plots Compared

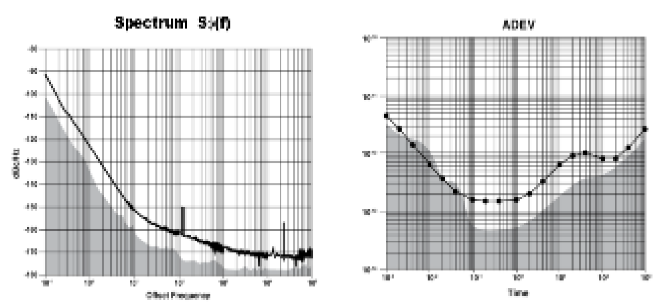

Fig. 3. Spectrum and Allan Deviation (ADEV) of NEL OCXO (Oven Controlled Crystal Oscillator). Instrumentation limits are shon in grey.

Asymptotes may be applied both to oscillator spectra and Allan Variance plots. And it is interesting to observe particularly how the corner-frequencies of the asymptotes on the two plots relate to each other. Also, how well the asymptotes can represent the spectra and corresponding ADEV plots. The spectrum shape and can be translated into Allan-variance plots by the kind of techniques indicated in Enrico Rubiola's Chart [7].

Fig.4 shows real measurements of an NEL OCXO which are used for determining the accuracy of the asymptotic representations.

Fig.5 shows asymptotes applied to both the Spectrum and ADEV plots but with ADEV plot reversed left to right as a mirror image. The plots are placed one above the other and have been aligned to give the best fit according to the assumption that the logarithmic time scale is the reciprocal of the logarithmic frequency scale.

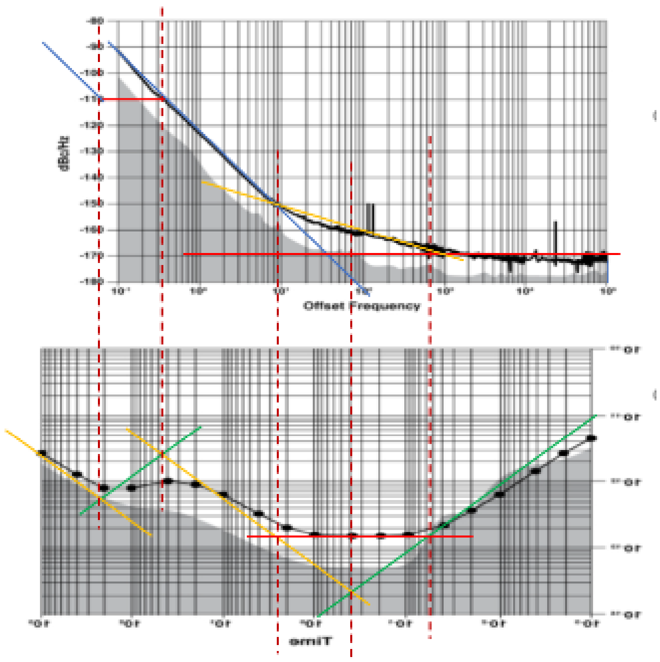

Fig. 4. Spectrum and mirror-image Allan Deviation (ADEV) plots of NEL OCXO aligned so that vertical red dashed lines show the correspondence of the asymptotic corner-frequencies in the two plots.

Fig. 5 shows that asymptotes can be used both on the $S_\phi(f)$ spectrum and on an ADEV plot. Slopes are constrained exactly to f^0 =+3dB green, 0 = 0dB red, f^{-1} =-3dB orange, and f^{-2} = -6dB blue per octave.

The ADEV plot has been reflected horizontally to attempt alignment of ADEV reciprocal time $1/\tau$ with f and the vertical dashed dark red lines indicate corresponding corner frequencies on the $S_\phi(f)$ and ADEV plots.

This shows that the general shapes can be correlated but some offsetting of different corners are required between the corners on the two plots and needs to be calculated and justified.

There is a surprising 1/f orange -3dB section on the $S_\phi(f)$ plot corresponding to red 0dB section on the ADEV Plot. It is also shown also on Enrico Rubiola's Chart [7]. The physics of this needs to be explained. At present no known oscillator model models this! A new oscillator model is needed.

Since when aligned the two plots in Fig. 5 do not completely overlap the frequency plot has been extended downwards on the assumption that the two plots are indeed connected and correlated.

Note that this part of the plots is shaped by the oven feedback loop characteristics of the OCXO.

VIII. Asymptotic ADEV Filter Shape .

The process of creating an ADEV can be likened to the application of an $\mathrm{Sin}^2\omega/\omega$ angular frequency (ω in radians per second) filter. An asymptotic approximation to this filter characteristic can be derived and this is shown three times on the (un-reflected) ADEV plot in Fig. 6. The interesting discovery is that this filter appears to retain exactly the same shape and dimensions for any value of the ADEV sample difference time τ.

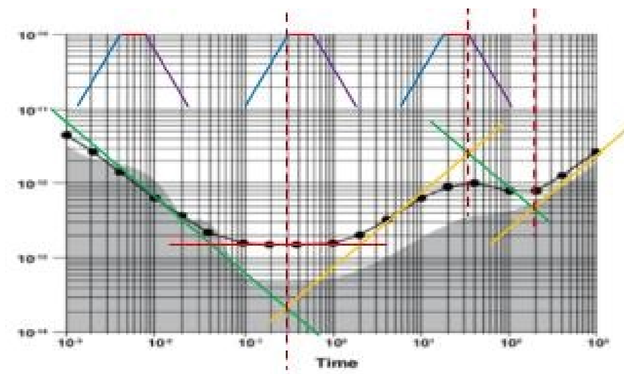

Fig. 5. Allan Deviation (ADEV) of NEL OCXO (Oven Controlled Crystal Oscillator) showing the constant shape and size of the ADEV filtering acion.

In Fig. 6 the slopes are contain the additional slope of f^{-2} or -6dB per octave in mauve.

IX. Conclusion

This work has made significant advances in the understanding and modelling of oscillators and their fundamental chaotic instabilities. New upgraded modelling equations have been presented indicating the presence of albeit small but irreducible chaotic spectrum and jitter instabilities.

Further work is needed to refine and calibrate the new proposals and perhaps further improve the rapidity and accuracy of oscillator measurements.

The eventual target is even better oscillator designs.

X. Conclusions

For oscillator design the 'Cool Model' is better than the 'Leeson Model' and should be used from now on in preference.

The 'Asymptotic Representation' usefully identifies the 'corner-frequencies' on plots of the phase-noise-spectrum, ADEV, $L_{LSB}(f)$, $L_{USB}(f)$ and $S_\phi(f)$.

The 'corner frequency' regions of both spectrum and ADEV plots are fundamentally unstable within a bandwidth of $\sim f/\pi$.

The instabilities are non-gaussian with expected 'chaotic' and 'metastable' statistics.

The maximum spectrum variation at the corner frequency is estimated to be ~1.5 dB which is small and not likely to appear on ADEV measurements particularly if averaging is used. And will not appear on spectrum measurements if averaging with 'outlier removal' is used.

The next oscillator model under consideration is the 'Cool-Physics Model' which will take into account that a spectrum has a temperature profile that is proportional to the spectral-density at every point and this can vary dynamically in time. But it may well only be of academic interest?

References

[1] D. B. Leeson, "A simple model of feedback oscillator noise spectrum," Proc. IEEE, vol. 54, no. 2, pp. 329–330, Feb. 1966.

[2] J. Everard, "Fundamentals of RF circuit design with low noise oscillators", .New York: Wiley, 2000, ISBN 0-471-49793-2.

[3] J. Everard, M. Xu, and S. Bale, "Simplified phase noise model for negative-resistance oscillators and a comparisonwith feedback oscillator models", IEEE TUFFC, vol. 59, no. 3, March 2012.

[4] M. J. Underhill, "Oscillator resistor noise optimisation paradigm" IFCS 2016, May 9-12, New Orleans, Louisiana pp. 1-5.

[5] M. J. Underhill, "Theory of Random Spurs and Spectrum-Collapse from SDR Phase-Noise and Carrier-Phase Measurements", IFCS 2018, Olympic Valley, CA, USA.

[6] M. J. Underhill, "The Cool Oscillator Model with Predicted Performance in Practical Systems with Explanations of Oscillator-Spurs and Injection-Locking Processes", Proceedings IFCS-ISAF 2020.

[7] E. Rubiola, "Enrico's Chart of Phase Noise and Two-Sample Variances", http://rubiola.org/pdf-static/Enrico's-chart-EFTS.pdf

[8] https://en.wikipedia.org/wiki/Laplace_transform

[9] https://en.wikipedia.org/wiki/Control_theory

[10] https://en.wikipedia.org/wiki/Transfer_function

[11] https://en.wikipedia.org/wiki/Inverse_Laplace_transform

[12] https://en.wikipedia.org/wiki/Partial_fraction_decomposition

[13] https://en.wikipedia.org/wiki/Bode_plot

Author References

[A1] M. J. Underhill, "Universal frequency synthesiser IC system". 1978 IEE Conference on Communications Equipment and Systems April 1978, pp.185-188.

[A2] M. J. Underhill, "Oscillator noise limitations", IERE Conference Proc. No. 39, Electromagnetic Compatibility, April 1978.

[A3] M. J. Underhill, "Transient and frequency responses of systems with time delays", IEE Electronics Letters, Vol. 14, No. 9, April 1978, pp. 284 – 286.

[A4] M. J. Underhill, P. A. Jordan, M. A. G. Clarke and R. I. H. Scott, "A general purpose LSI frequency synthesiser system". Proceedings of 32nd Annual Symposium on Frequency Control 1978, Atlantic City, NJ, USA (US Army Electronics Command, Fort Monmouth, NJ), pp.365-372.

[A5] M. J. Underhill, P. A. Jordan, and M. Sarhadi, "Fast digital frequency synthesiser" Electronics Letters 25 May, 1978, Vol. 14, No. 11. pp.342-343.

[A6] M. J. Underhill, M. Sarhadi, and C. S. Aitchison, "Fast sampling frequency meter", Electronics Letters, 8 June 1978, Vol. 14, No. 12, pp. 366-367.

[A7] M. J Underhill, "Comparison of the noise performance of some oscillators for tunable receivers", IERE Conference Proceedings No. 40, Radio Receivers and Associated Systems, Southampton July 1978, pp.237-252.

[A8] M. Sarhadi, C. S. Aitchison and M. J. Underhill, "A fast sampling microwave frequency counter". Proceedings of 8th European Microwave conference, Paris, September 1978, pp. 519-523.

[A9] M. J. Underhill, and R. I. H. Scott, "The effect of the sampling action of phase comparators on frequency synthesiser performance". Proceedings 33rd Annual Symposium on Frequency Control 1979 - 30th May/1st June 1979. Fort Monmouth NJ, USA (held at Atlantic City) pp.449-457.

[A10] M. J. Underhill, and P. A. Jordan, "Split-loop method for wide-range frequency synthesiser with good dynamic performance". Electronics Letters, 21st June 1979, Vol. 15, No. 13, pp.391-393.

[A11] M. J. Underhill and R. I. H. Scott, "Wideband frequency modulation of frequency synthesisers", Electronics Letters, 21st June 1979, Vol. 15. No. 13, pp.393-394.

[A12] M. J. Underhill, "Wide range frequency synthesisers with improved dynamic performance" IERE Conference on Land Mobile Radio, Lancaster, September 1979, pp.171-182.

[A13] R. I. H. Scott and M. J. Underhill,, "FM modulation of frequency synthesisers", IERE conference on Land Mobile Radio, Lancaster, September 1979, pp.183-191.

[A14] M. J. Underhill, Chapter 4 of "Radio Receivers" edited by William Gosling, IEE Telecommunication Series, published by Peter Peregrinus Ltd., 1986, ISBN: 0-86341-056-1.

[A15] M. J. Underhill, "Fundamental limitations of oscillator performance", IEE Conf. Publ. 303, Frequency control and synthesis, 1989, pp 18-31.

[A16] M. J. Underhill, "Fundamentals of oscillator performance", Electronics & Communication Engineering Journal Volume: 4, Issue: 4, 1992, pp. 185–193.

[A17] M. J. Underhill, "The magic of marginal electronics", Electronics & Communication Engineering Journal, Vol. 5, No. 6, Dec

[A18] M. J. Underhill and M. J. Blewett, "Spectral improvement of direct digital frequency synthesisers and other frequency sources", 10th European Frequency and Time Forum, 1996, EFTF 96, 5-7 March (IEE Conf. Publ. 418) pp. 452-460.

[A19] M. J. Underhill, "Reduction of phase noise in single transistor oscillators", 10th European Frequency and Time Forum, 1996, EFTF 96, 5-7 March (IEE Conf. Publ. 418), pp. 476- 490

[A20] M. J. Underhill and M. J. Blewett, "Phase Noise and Time Jitter Reduction Circuit". Microwaves & RF Conference, 8-10 October 1996, London, pp.361-366.

[A21] M. J. Underhill and M. J. Blewett, "Phase Noise and Time Jitter Reduction Circuit". Microwaves & RF Conference, 8-10 October 1996, London, pp.361-366.

[A22] M. J. Underhill and M. J. Blewett, "Performance Assessment of a Delay Compensation Phase Noise and Time Jitter Reduction Method", 11th European Frequency and Time Forum, Neuchatel, Switzerland, 5 - 7 March 1997, pp.364-368.

[A23] M. J. Underhill and M. J. Blewett, "Spectral Improvement of Direct Digital Frequency Synthesizers and other Frequency Sources", 11th European Frequency and Time Forum, Neuchatel, Switzerland, 5-7 March 1997, pp.452-460.

[A24] M. J. Underhill, "Reduction of Phase Noise in Single Transistor Oscillators", 11th European Frequency and Time Forum, Neuchatel, Switzerland, 5 - 7 March 1997, pp.476-490.

[A25] M. J Underhill, S, Stavrou, M. J Blewett,. and N. Downie, "The Anti Jitter Circuit for low spurious DDS square waves and low cost fractional-n synthesis". 12th European Frequency and Time Forum, EFTF Warsaw, March 1998, pp.292-297.

[A26] M. J. Underhill, "The high gain phase comparator for reduction of close-to-carrier phase noise", 12th European Frequency and Time Forum, EFTF Warsaw, March 1998, pp.215-221.

[A27] M. J. Underhill, "The Anti Jitter Circuit for the Suppression of Wideband Phase-Noise", 1998 IEE Colloquium on 'Microwave and Millimetre-Wave Oscillators and Mixers' (Ref. No. 1998/480), pp. 2/1 - 2/14

[A28] M. J. Underhill, "The Adiabatic Anti Jitter Circuit", Joint Meeting of the 12th European Frequency and Time Forum, EFTF, and 1999 IEEE Frequency Control Symposium April 1999,

[A29] M. J. Underhill, "The Adiabatic Anti Jitter Circuit", Joint Meeting of the 12th European Frequency and Time Forum, EFTF, and 1999 IEEE Frequency Control Symposium April 1999.

[A30] K. S. Ang, M. J. Underhill and I. D. Robertson, "Transmission Line Stabilised Oscillators". Proceedings 14th EFTF 2000, 14-16 March, Torino, Italy, pp. 88-92.

[A31] M. J. Underhill, “Phase Noise Limits of the Anti-Jitter Circuit and On-Chip RC Oscillators”. Proceedings 14th EFTF 2000, 14-16 March, Torino, Italy, pp. 138-142

[A32] K. S. Ang, M. J. Underhill and I. D. Robertson, “Balanced monolithic oscillators at K- and Ka-band”, IEEE Transactions on Microwave Theory and Techniques, 2000, Volume: 48, Issue: 2, pp. 187-193.

[A33] K. S. Ang, M. J. Underhill and I. D. Robertson, “Transmission Line Stabilised Oscillators”. Proceedings 14th EFTF 2000, 14-16 March, Torino, Italy, pp. 88-92.

[A34] M. J. Underhill, “Phase Noise Limits of the Anti-Jitter Circuit and On-Chip RC Oscillators”. Proceedings 14th EFTF 2000, 14-16 March, Torino, Italy, pp. 138-142

[A35] K. S. Ang, M. J. Underhill and I. D. Robertson, “Balanced monolithic oscillators at K- and Ka-band”, IEEE Transactions on Microwave Theory and Techniques, 2000, Volume: 48, Issue: 2, pp. 187-193.

[A36] M. J. Underhill, “The adiabatic anti-jitter circuit”, IEEE Transactions on Ultrasonics, Ferroelectrics, and Frequency Control 2001, Volume: 48, Issue: 3, pp. 666- 674.

[A37] N. Siripon, M. J. Underhill, and I. D. Robertson, “Reduced spurious signals in an injection-locked oscillator by using combining technique”, 33rd European Microwave Conference 2003, pp. 507-510.

[A38] M. J. Underhill, “The noise and suppression transfer functions of the Anti-Jitter circuit”, Proceedings of the 2003 IEEE International Frequency Control Symposium and PDA Exhibition Jointly with the 17th European Frequency and Time Forum, 2003, pp. 490-498.

[A39] S. Bunnjaweht, M. J. Underhill and I. D. Robertson, “Sideband noise reduction in transposed gain oscillators”, Proceedings of the 2003 International Symposium on Circuits and Systems. ISCAS '03, Vol. 1, pp. 713-716.

[A40] N. Siripon, M. J. Underhill, and I. D., Robertson, “Reduced spurious signals in an injection-locked oscillator by using combining technique”, 33rd European Microwave Conference 2003, pp. 507-510.

[A41] M. J. UnderhillS. Bunnjaweht, M. J. Underhill and I. D. Robertson, “Novel jitter and phase noise reduction circuit”, 18th European Frequency and Time Forum, 2004. EFTF 2004, pp. 300-303.

[A42] S. Bunnjaweht, M. J. Underhill and I. D. Robertson, “IF-LO delay mismatch and noise reduction in transposed gain oscillators”, 18th European Frequency and Time Forum, 2004. EFTF 2004, pp. 509-512.

[A43] M. J. Underhill and P. J., Brown, “Estimation of total jitter and jitter probability density function from the signal spectrum”, 18th European Frequency and Time Forum. EFTF 2004, pp. 502- 508.

[A44] M. J. Underhill and J. Brodrick, “The performance of the anti-jitter circuit with enhanced feedback ('EF-AJC')”, Proceedings of the 2004 IEEE International Frequency Control Symposium and Exposition, 2004, pp. 158-164.

[A45] M. J. Underhill, “Asymmetric spectra of phase modulated transitions of square waves”, European Frequency and Time Forum (EFTF), 2012 pp. 509-513.

[A46] M. J. Underhill, “Time jitter and phase noise — Now and in the future?”, 2012 IEEE International Frequency Control Symposium Proceedings, pp. 1-8.

[A47] M. J. Underhill, “Investigation into spectrum shape fluctuations of oscillators and signal sources”, 2013 Joint European Frequency and Time Forum & International Frequency Control Symposium (EFTF/IFCS), 2013, 729-732.

[A48] M. J. Underhill, “Coupling theory for fluctuating spurs in oscillators”, IFCS 2014, May 19-22, Taipei, Taiwan, pp. 1-5.

[A49] M. J. Underhill, “Oscillator resistor noise optimisation paradigm” IFCS 2016, May 9-12, New Orleans, Louisiana pp. 1-5.

[A50] M. J. Underhill, “Propagation frequency shifts and impact on time and frequency transfer and gravity wave detection”, IFCS 2016, May 9-12, New Orleans, Louisiana.

[A51] M. J. Underhill. “The Two-Edge Anti-Jitter Circuit for Phase Noise Reduction on Received Frequency Standards”, Joint Conf. EFTF/IFCS 2017, Besancon, France, pp. 117 – 120.

[A52] M. J. Underhill, “Observed propagation-phase/frequency-shift theory with impact on time/frequency transfer, GNSS and Gravity Waves”, Joint Conf. EFTF/IFCS 2017, Besancon, France, pp. 733 – 735.

[A53] M. J. Underhill, “Measuring small propagation frequency shifts and fluctuations by phase to avoid cross-correlation errors”, EFTF 2018, Turin, Italy.

[A54] M. J. Underhill, “Theory of Random Spurs and Spectrum-Collapse from SDR Phase-Noise and Carrier-Phase Measurements”, IFCS 2018, Olympic Valley, CA, USA.

[A55] M. J. Underhill, “The Cool Oscillator Model with Predicted Performance in Practical Systems with Explanations of Oscillator-Spurs and Injection-Locking Processes”, Proceedings IFCS-ISAF 2020.